Fracture of concrete beams at different loading rates

H.W. Reinhardt, J. Ožbolt
Department of Construction Materials, University of Stuttgart, Germany

ABSTRACT: To investigate the influence of the loading rate on the cracking behavior of plain concrete beams, a 3D finite element analysis of notched three-point bending beams (normal strength concrete) and cantilever beams (normal and high strength concrete) was carried out. In the used finite element code a model, which is applicable over a many orders of magnitude of the loading rate was adopted. The model is based on the rate process theory of bond ruptures. It was coupled with the microplane model for concrete. Both, static and dynamic analyses were performed. The static analysis was performed using an implicit type of approach whereas in the dynamic analysis the explicit direct integration method was employed. The results show that the loading rate significantly influences the peak resistance and the failure mode of concrete beams.

1 INTRODUCTION

It is well known that loading rate significantly influences the structural response. The structural response depends on the loading rate through three different effects: (1) through the creep of the bulk material between the cracks, (2) through the rate dependency of the growing microcracks and (3) through the influence of inertia forces, which can significantly change the state of the stresses and strains at the crack tip. Depending on the type of material and the loading rate, the first, second or third effect may dominate. For quasi-brittle materials, such as concrete, which exhibit cracking and damage phenomena, the first effect is important for relatively low loading rates (creep-fracture interaction). However, the later two effects dominate for higher loading rates and these are considered in this paper. The behavior of notched plain concrete beams loaded by three-point bending and cantilever beams with different loading rates was numerically investigated. The loading rate was varied from slow to very fast (impact). To demonstrate the influence of the loading rate on the size effect, beams of three different sizes were analyzed. The three-dimensional (3D) finite element (FE) analysis was performed by employing the rate dependent microplane model for concrete.

2 RATE DEPENDENT CONSTITUTIVE LAW FOR CONCRETE

The rate dependency in the here used microplane model for concrete (Ožbolt et al., 2001) considers the rate dependency related to the formation of the microcracks. The influence of inertia forces on the rate effect is not a part of the constitutive law, however, this effect is automatically accounted for in dynamic finite element analyses in which the constitutive law interacts with inertia forces.

For moderately high loading rates the concrete response is controlled by the rate of growing microcracks. Based on the activation energy theory (Krausz & Krausz 1988), the influence of the rate of growing microcracks on the rate independent microplane stress-strain relation $\sigma_M^0(\varepsilon)$ can be written as (Bažant et al., 2000; Ožbolt & Rah 2005):

$$\sigma_M\left(\varepsilon_M\right) = \sigma_M^0\left(\varepsilon_M\right)\left[1 + c_2 \ln\left(\frac{2\dot{\gamma}}{c_1}\right)\right]$$

$$\text{with} \quad \dot{\gamma} = \sqrt{\frac{1}{2}\dot{\varepsilon}_{ij}\dot{\varepsilon}_{ij}} \;;\; c_1 = \frac{c_0}{s_{cr}} \tag{1}$$

where c_0 and c_2 are material rate constants which have to be calibrated by fit of the test data, $\dot{\varepsilon}_{ij} =$ components of the macroscopic strain rate tensor (indicial notation), M stays for the microplane volumetric, deviatoric and shear components of stresses,

respectively (Ožbolt et al., 2001). The above parameters were calibrated based on the uniaxial compressive tests (Ožbolt & Rah 05). The calibration of the constitutive law was carried out for moderate loading rates for which inertia forces have not much influence on the rate dependent response of the material, i.e. only the rate of the crack growth controls the response.

3 3D FE STATIC AND DYNAMIC ANALYSES

The rate sensitive microplane model is used together with the crack band method (Bažant & Oh 1983) in the here presented 3D FE analysis of plain concrete beams. Static analysis is performed using an implicit 3D FE code that is based on the incremental secant stiffness approach. In the 3D transient dynamic FE analysis the system of unknown displacements is for each time step Δt calculated by solving the following system of equations (Voigt notation):

$$\mathbf{M}\ddot{\mathbf{u}}(t) + \mathbf{C}\dot{\mathbf{u}}(t) - \mathbf{f}(t) = 0 \qquad (2)$$

where $\mathbf{M}$ = mass matrix, $\mathbf{C}$ = damping matrix, $\ddot{\mathbf{u}}$ = nodal accelerations, $\dot{\mathbf{u}}$ = nodal velocities and $\mathbf{f}(t)$ = resulting nodal forces. The resulting nodal forces are calculated as:

$$\mathbf{f}(t) = \mathbf{f}^{\text{ext}}(t) - \mathbf{f}^{\text{int}}(t) \qquad (3)$$

with $\mathbf{f}^{\text{ext}}(t)$ = external nodal forces; $\mathbf{f}^{\text{int}}(t)$ = internal nodal forces.

The above system of equations (2) is solved using direct integration scheme of explicit type (Bažant & Oh 1983). The external nodal forces are known nodal loads. The internal nodal forces are unknown and they are calculated by the integration of the stresses over the finite elements. In the used FE code mass matrix and damping matrix are taken as diagonal. The direct integration procedure of explicit type is stable if the time step Δt is smaller or equal than the critical one (Belytschko et al. 2001), i.e.:

$$\Delta t \leq \Delta t_{\text{crit}} \qquad (4)$$

The stability of the analysis is controlled by the energy balance check (Belytschko et al. 2001). Because of the conservation of energy the total energy introduced into the FE model must be equal to the sum of the potential and kinetic energy:

$$\left| W_{\text{kin}} + W_{\text{int}} - W_{\text{ext}} \right| \leq \lambda \cdot \max(W_{\text{kin}}, W_{\text{int}}, W_{\text{ext}}) \qquad (5)$$

where W_{kin}, W_{int} and W_{ext}, are kinetic, internal (potential) and external energy, respectively. The tolerance λ is typically set to 0.01.

4 INFLUENCE OF THE LOADING RATE ON THE FAILURE OF NOTCHED PLAIN CONCRETE BEAMS

To investigate the influence of the loading rate on the response of notched plain concrete beams, loaded in three-point bending, a 3D FE analysis was performed. For each loading rate three beam sizes were analysed (beam depth h = 50, 200 and 400 mm). The width of the beam was for all beam sizes the same and equal b = 5 mm. In a 2D plane the beams were proportionally scaled. The span-depth ratio and the relative notch depth were taken as L/h = 4 and a/h = 1/5, respectively. The rate independent properties of concrete were taken as: Young's modulus E_C = 30000 MPa, Poisson's ratio ν_C = 0.18, tensile strength f_t = 2 MPa, uniaxial compressive strength f_c = 30 MPa and concrete fracture energy G_F = 0.1 N/mm. Mass density of the concrete was set to ρ = 2.3 t/m^3. In the analysis the plane strain state was assumed. The load was performed by controlling the mid-span displacement of the beam in vertical direction. The loading rate for all beam sizes was varied from 0.2 mm/sec to 2 x 10^4 mm/sec. Static and dynamic analysis was performed. In static analysis the implicit secant stiffness approach was applied. In dynamic analysis direct integration of explicit type was used. To avoid local oscillations of the finite elements, damping was set to 0.023 N sec/mm. Static analysis was performed for all loading rates. Dynamic analysis was carried out for loading rates larger than 0.2 mm/sec. To eliminate mesh size sensitivity the crack band method was used.

4.1 *Results of static analysis*

The typical calculated load-displacement curves (h = 200 mm) for different loading rates are shown in Fig. 1a. As can be seen, with increase of the loading rate the peak load and the initial stiffness increase. The failure mode is due to Mode-I fracture (Fig. 1b) and it is independent of the loading rate. The relation between the calculated relative nominal strength σ_N/f_t ($\sigma_N = 6M_U/(bh^2)$, $M_U = P_U L/4$) and the loading rate is plotted for all beam sizes in Fig. 2a. It can be seen that with increase of the loading rate the nominal bending strength increases.

It is known that with the decrease of the loading rate from relatively fast (approximately 1 sec up to the peak load) to very slow (approximately 1.0 x 10^4 sec up to the peak load) the size effect on the nominal strength becomes stronger, i.e. the characteristic size (h_0) of the beam decreases with decrease of the loading rate. The reason for this is creep-fracture interaction (Bažant & Planas, 1998), which causes higher brittleness of a concrete beams (smaller characteristic size).
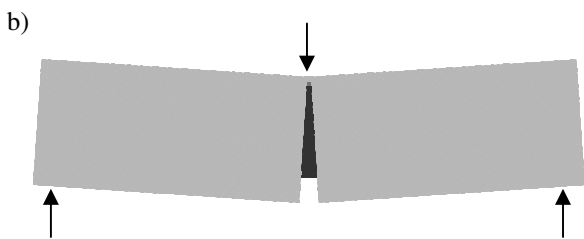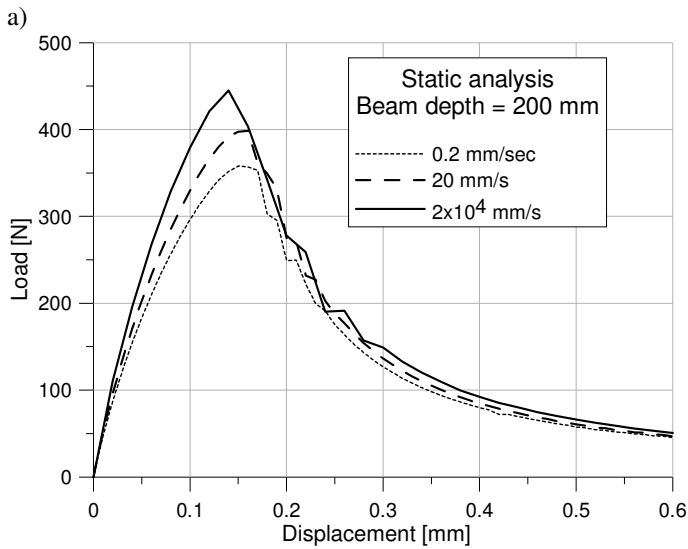
a)

b)

Figure 1. Static analysis: (a) Typical load-displacement curves for different loading rates (h = 200 mm); (b) Typical bending (Mode-I) failure type

Note, that for $h < h_0$ the behaviour of the beam is close to plasticity (no size effect) and for $h > h_0$ the beam response is closer to the prediction according to LEFM (maximal size effect). The results of the finite element analysis principally confirm this observation. If the loading rate is larger than the usual, the characteristic beam size decreases. This indicates the existence of the loading rate for which the size effect is minimal (the largest characteristic size). The size critical loading rate depends on the problem type and material properties.

4.2 *Results of dynamic analysis*

To investigate the influence of inertia forces on the rate dependent response of the notched concrete beams, the above analysis was repeated, however, the analysis was dynamic. The relation between the calculated relative nominal strength and the loading rate is for all beam sizes plotted in Fig. 2a. It can be seen that, the same as in static analysis, with increase of the loading rate the nominal bending strength increases. However, for very high loading rates there is progressive increase of the nominal strength after the loading rate reaches a critical value.
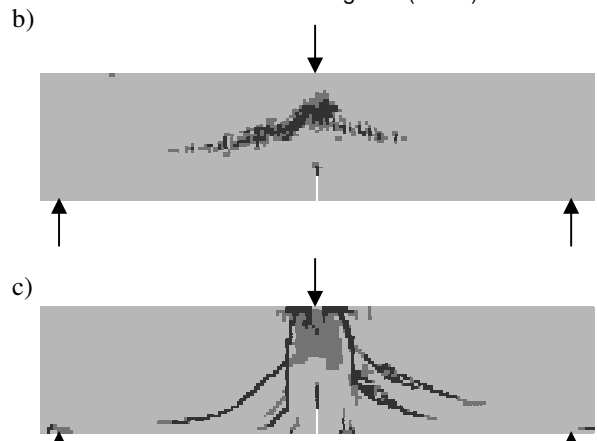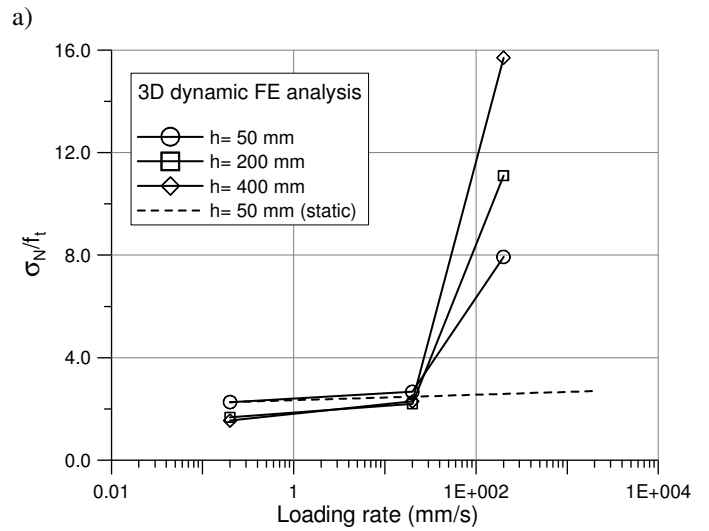
a)

b)

c)

Figure 2. Dynamic analysis: (a) Influence of the loading rate on the nominal strength; (b) Horizontal splitting-shear failure; c) Mixed mode failure type

This is due to the influence of inertia forces, which is larger if the beam is larger. For loading rates greater than 10 mm/sec the inertia forces dominate. The failure mode is dependent on the loading rate. For the loading rate between 0.1 and 10 mm/sec the failure is caused by the horizontal separation of the beam (see Fig. 2b). Finally, for very high loading rates the failure is due to mixed mode failure type (see Fig. 2c).

5 NUMERICAL STUDY OF CANTILEVER BEAM

5.1 *Geometry and material properties*

Static and dynamic fracture of the cantilever beam was studied on a beam with length $L = 500$ mm, height $H = 200$ mm and thickness $D = 10$ mm. Plane strain was assumed, i.e. only one row of 3D finite elements over the thickness of the beam was considered. The load was applied at the free end of the cantilever by controlling vertical displacement. Totally six loading rates were considered: $d\delta/dt =$ 2.0E10[4], 2.0E10[3], 2.0E10[2] and 20, 2 and 0 mm/s. To prevent local failure of concrete under the applied load, four

elements under the applied load were taken as linear elastic. Full contact between the load and the beam surface was assumed. Static and dynamic analyses were carried out for the same loading rates and for two concrete types, i.e. for the normal strength concrete (NSC) and for the high performance fiber reinforced concrete (ECC). The material properties for both concretes are shown in Figure 3. The corresponding stress-strain curves for uniaxial tension and compression are also shown. The curves are related to the size of the finite element of $h = 10$ mm. The high performance fiber reinforced concrete used in the study is the concrete with high ductility (Li 2002). In contrast to the normal strength concrete, for this concrete the average ultimate tensile strain in uniaxial tensile fracture test reaches more than 5% and damage (cracking) at failure is distributed over the entire volume of the test specimen.

In the finite element analysis solid eight nodes elements were used. Damping was set to zero except in the analysis of ECC beams loaded by lower loading rates ($d\delta/dt$ = 2, 20 and 200 mm/s) where the damping was set to 0.023 [N s/mm]. This appeared to be necessary because of numerical reasons, i.e. to get the explicit integration algorithm stable. Mass density for both concrete types was taken as $\rho = 2.30$ t/m^3.
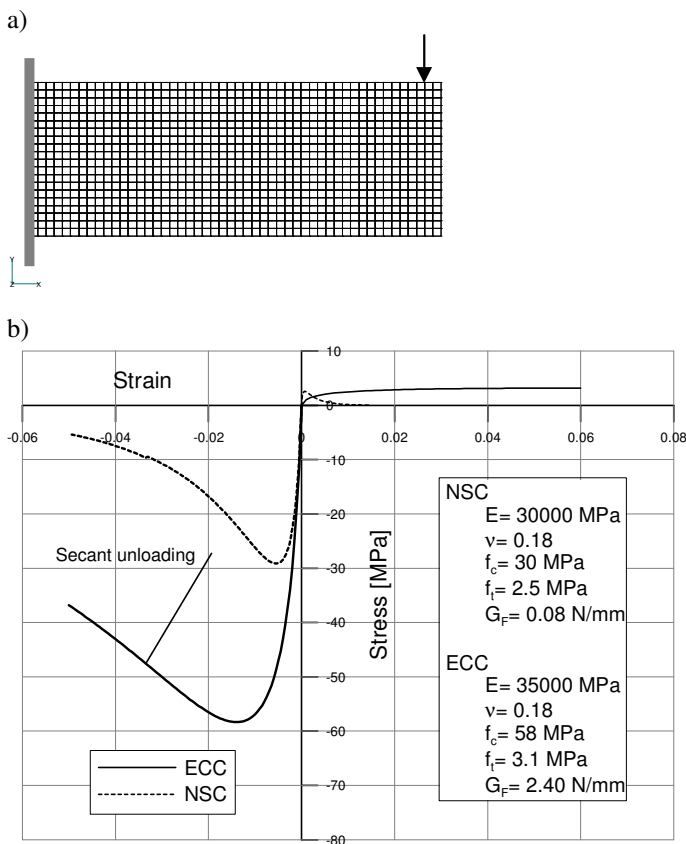
a)

b)

Figure 3. Cantilever: (a) Geometry and (b) Material properties – NSC & ECC concrete

5.2 Results for NSC Beam

Calculated load-displacement curves obtained for static loading with different loading rates are shown in Figure 4a. As expected, by increase of loading rate, the peak load and the initial stiffness increase. The peak load for the highest loading rate ($d\delta/dt$ = 2.0E+04) is 52% larger than the peak load for the static load with no rate effect ($d\delta/dt$ = 0). The typical failure mode is Mode I, i.e. bending failure at the support. This failure mode is obtained for all loading rates applied in the static analysis.

One example of the load-displacement curves from dynamic analysis is plotted in Figure 5. The horizontal and the vertical reactions (R_X and R_Y), calculated as a sum of horizontal and vertical nodal forces over the fixed end of the beam, and the total external load (P), applied at the cantilever end, are plotted as a function of the prescribed displacement δ. It can be seen that the vertical reaction load is delayed and is much smaller than the applied load. Furthermore, a relatively large horizontal reaction R_X is obtained. The axial load is compressive and during loading it does not change sign.

For relative slow loading ($d\delta/dt$ = 2, 20 and 200 mm/s) the failure mode is the same as in the static analysis, i.e. Mode I fracture due to bending. However, for $d\delta/dt$ = 2.0E+04 mm/s the beam fails in the region under the applied load due to diagonal shear (Mixed-mode) (Fig. 6). It is interesting to observe that the rest of the beam remains almost stress free. This can be clearly seen from Figure 5, which shows that at maximal load the reaction forces are practically zero. Such a response is possible because of very high loading rate, which in the local region under the applied load generates high inertia forces, which are in equilibrium with the applied load. Once the beam fails in shear (softening part of the load-displacement curve) the stress wave progresses to the support direction and generates relatively high compressive and shear forces at the beam support (see Figure 5).
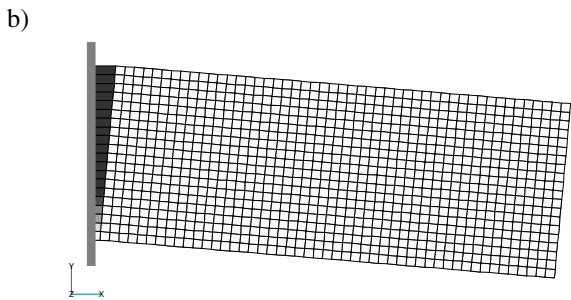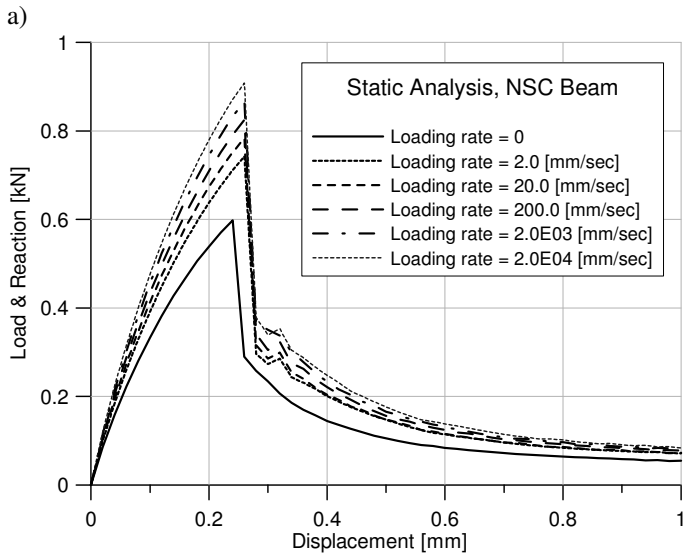
a)

b)

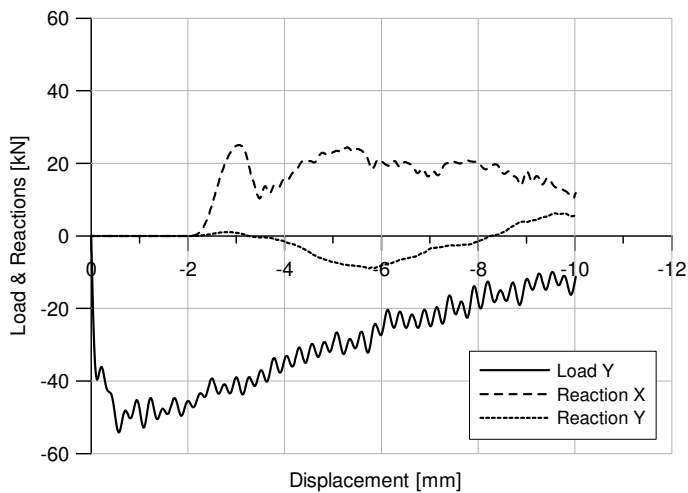Figure 4. NSC beams, static analysis: (a) calculated load-displacement curves and (b) typical failure mode.

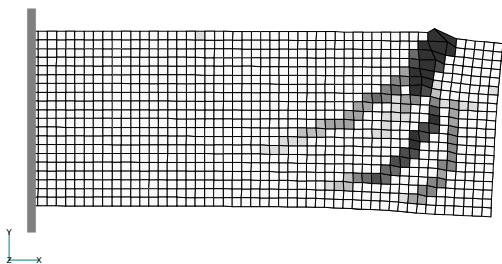Figure 5. NSC beam, dynamic analysis – load and reactions versus prescribed displacement for loading rate= 2E+04 mm/s.

Figure 6. NSC Beams, dynamic analysis: failure mode for the highest loading rate (2E+04 mm/s).

5.3 *Results for ECC Beam*

The calculated load-displacement curves for static and dynamic analysis are plotted in Figure. 7 and Figure 8, respectively. Apart from the shape of the curves, which exhibit more ductile response than those obtained for NSC beams, and apart from the differences in the peak loads, the effect of the loading rate is similar to that of NSC beams. Moreover, the failure modes obtained in the static (see Figure 7b) and dynamic analysis (see Figure 9) are principally the same as discussed for NSC. The only one difference is that damage tends to be distributed over a larger volume of the beam rather than to be localised. The reason for this is high ductility of ECC which makes redistribution of stresses possible and results in higher resistance.
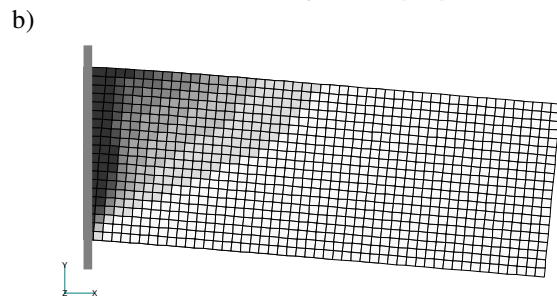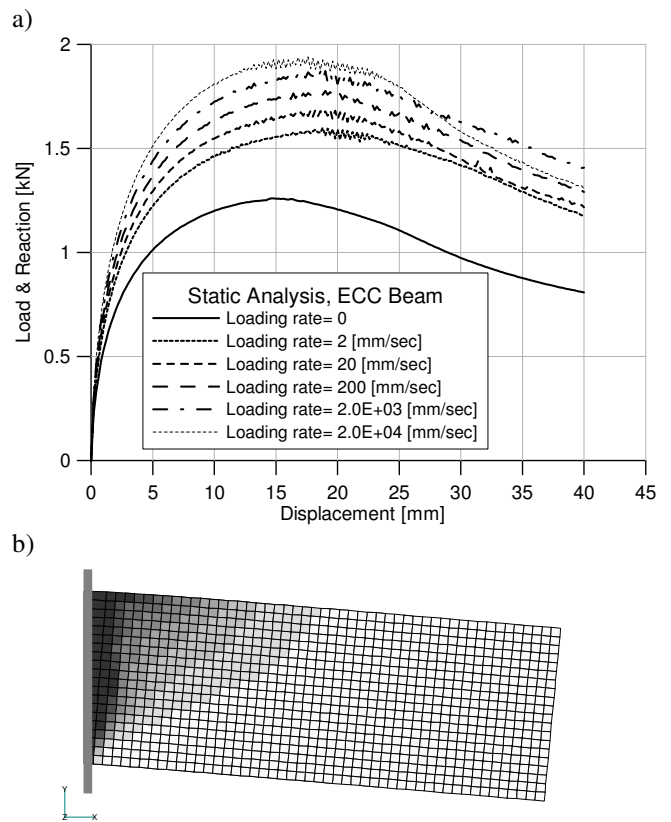
a)

b)

Figure 7. ECC beams, static analysis: (a) calculated load-displacement curves and (b) typical (bending) failure mode.
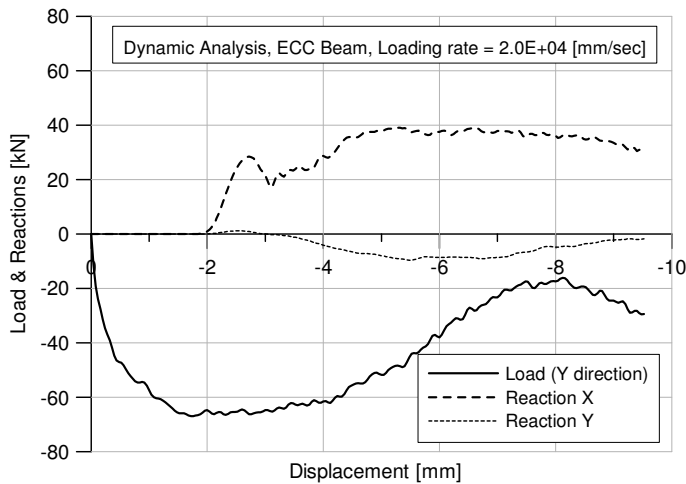
Figure 8. ECC beams, dynamic analysis – load and reactions versus prescribed displacement for loading rate= 2E+04 mm/s.
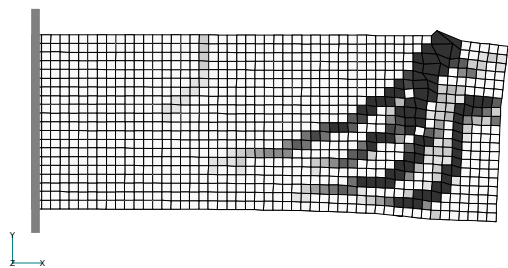

Figure 9. ECC Beams, dynamic analysis failure mode obtained for the highest loading rate (2E+04 mm/s).

5.4 *Discussion of the results*

Comparing the results of the static and dynamic analysis it is obvious that for NSC and ECC beams loading rate significantly influence the beam response. The higher loading rates lead to higher resistance. The relations between the loading rate and relative beam resistances are plotted in Figure 10. For static load the loading rate has slightly more effect on the resistance of ECC beams (see Figure 10a). Compared to the static loading with no rate effect (very slow loading) the peak load for the highest loading rate of ECC beam increases by 55%. The corresponding increase for NSC beam is 52%. It can be seen that in the log scale the relative beam resistance is practically linear proportional to the loading rate. Furthermore, it can be seen that the resistance of the ECC beam for static loading is roughly two times higher than the resistance of NSC beams although the tensile strengths for both concretes are similar (2.5 MPa vs. 3.1 MPa). The difference is due to the contribution of the fracture energy to the resistance, which is in the case of ECC many times higher.

For dynamic loading the effect of the loading rate on the maximal load is enormous (see Figure 11b). Compared to the peak resistance of the lowest static loading rate, the maximal load is about 90 (NSC) and 50 (ECC) times larger.

The results of the numerical study show that the type of the analysis (static or dynamic) can lead to significantly different structural response. Only for moderately large loading rates the results of static and dynamic analysis are comparable. For such loading rates bond rupture controls the effect of the strain rate on the beam response. However, for very high loading rates inertia forces become important. The effect of inertia forces can not be filtered out from the test result. Therefore, when the rate sensitive model needs to be calibrated, it is important to perform dynamic analysis in order to account for the effect of inertia forces on the response of the test specimen. Otherwise the model is not objective for the entire range of the strain rates. Further numerical studies are needed to investigate the influence of inertia forces on the response of concrete cantilever beam.
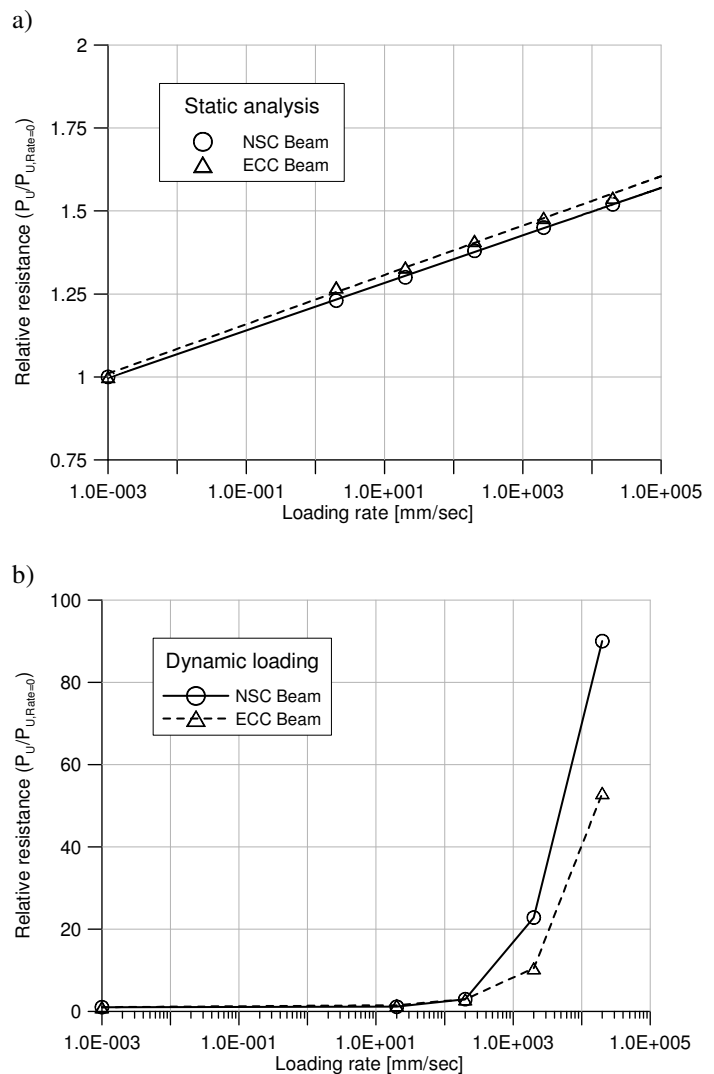
a)

b)

Figure 10. Influence of the loading rate on the ultimate load: (a) static loading and (b) dynamic loading.

6 CONCLUSIONS

Based on the results of the numerical studies the following conclusions can be drawn. With increase of the loading rate the resistance increases. At mod-

erately high loading rates the response is controlled by rate dependent crack growth, however, for extremely fast loading (impact) the inertia forces dominate and all another influences can be neglected. Depending on the loading rate, three different failure modes of single spam beams can be observed: bending failure (slow and fast loading), horizontal splitting-shear failure (moderately fast loading) and mixed mode failure (very fast loading).

Also for the cantilever beams there is an increase of resistance due to high loading rates. For static loading failure is always due to bending. In dynamic analysis with relatively low loading rates failure mode and resistance of the beam is similar to that obtained for static loading, i.e. the beam fails in bending (Mode-I fracture). However, independent of the concrete type, in dynamic analysis with higher loading rates beams fail in diagonal shear (Mixed-mode fracture). Moreover, there is a relatively strong axial compressive action, which significantly contributes to the shear resistance of the beam. Because of the strong axial action obtained in the dynamic analysis with high loading rates, the differences in the ultimate capacity of ECC and NSC beams become less pronounced. For high loading rates the type of the analysis (static or dynamic) can have significant influence on the results. This is due to inertia forces, which at high loading rates become very important. Further studies are needed to investigate the influence of inertia forces on the response of the beam loaded high loading rates.

REFERENCES

Bažant, Z. P. and Planas, J., *Fracture and Size Effect in Concrete and Other Quasibrittle Materials*, Ed. W.F. Chen, Purdue University, 1998.

Bažant, Z. P., and Oh, B. H. 1983. "Crack band theory for fracture of concrete," *RILEM*, 93(**16**), 155-177.

Bažant, Z. P., Caner, F.C., Adley, M. D. and Akers, S. A., "Fracturing rate effect and creep in microplane model for dynamics", *Journal of Engineering Mechanics*, *ASCE*, 1126(**9**), 2000, p. 962-970.

Belytschko T., Liu W.K., and Moran M. 2001. "Nonlinear Finite Elements for Continua and Structures," John Wiley & Sons Ltd.

Krausz, A. S. and Krausz, K. 1988. "Fracture kinetics of crack growth," Kluwer, Dordrecht, The Netherlands.

Li, V.C. 2002. "Reflections of the Research and Development of Engineered Cementitious Composites (ECC)," *Proceedings of JCI International Workshop on Ductile Fiber Reinforced Cementitious Composites (DFRCC)*, Gifu, Japan: Japan Concrete Institute, 1-22.

Ožbolt, J. and Rah, K. K., "*Influence of loading rate on concrete cone failure*", submitted for possible publication *International Journal of Fracture*, 2005.

Ožbolt, J., Li, Y.-J. and Kožar, I., "Microplane model for concrete with relaxed kinematic constraint", *International Journal of Solids and Structures*, 38:,2001, p. 2683-2711.